ELSEVIER

Chemical Geology 192 (2002) 183–194

CHEMICAL GEOLOGY
INCLUDING
ISOTOPE GEOSCIENCE

www.elsevier.com/locate/chemgeo

Pitfalls in the determination of empirical dissolution rate equations of minerals from experimental data and a way out: an iterative procedure to find valid rate equations, applied to Ca-carbonates and -sulphates

Alexander A. Jeschke, Wolfgang Dreybrodt *

Karst Processes Research Group Bremen, Institute of Experimental Physics, University Bremen, Postfach 330410 NW1 Otto Hahn Allee 1 Bremen, Germany

Received 10 June 2001; accepted 17 June 2002

Abstract

Empirical rate equations such as $R=k(1-c/c_{eq})^n$ in the dissolution of minerals are common in nature, e.g. limestone. The quantity c is the concentration of a major ion contained in the mineral, and c_{eq} its concentration at equilibrium. If experimental data obey such a rate equation, by plotting $\log(R)$ versus $\log(1-c/c_{eq})$ straight lines are found from which k and n can be determined. In many experiments, however, especially for natural minerals c_{eq} is not known exactly. If one uses wrong values of c_{eq} that deviate only a few percent from true equilibrium such plots are severely distorted and one may conclude that above some value c_s the true order n changes to a new value, even when a rate equation as given above is valid. We present an iterative computational procedure, which allows to find the valid rate equation from experimental data, even when c_{eq} is not known. The method is applied to limestone and synthetic calcite as well as to natural and synthetic gypsum. New experimental data are given for the dissolution rates of anhydrite ($CaSO_4$). By use of our new method, we find that this mineral exhibits a surface controlled rate equation with $k=5.0\pm1.0\times10^{-6}$ mmol cm^{-2} s^{-1}, $n=4.5\pm0.2$ and $c_{eq}=23.5\pm0.1$ mmol/l at $T=10$ °C.

Keywords: Kinetics; Dissolution; Gypsum; Limestone; Anhydrite

1. Introduction

Dissolution processes of minerals in aqueous environments play a role of utmost importance in the evolution of geochemical systems. It is therefore mandatory to investigate dissolution rates in the laboratory to find their dependence on the chemical composition of the solution. Most simple linear rate equations are exhibited in the dissolution of rocksalt (Alkattan et al., 1997), expressed by

$$R = k\left(1-\frac{c}{c_{eq}}\right) \quad (1)$$

* Corresponding author. Tel.: +49-421-2183556; fax: +49-421-2187318.
E-mail address: dreybrod@physik.uni-bremen.de (W. Dreybrodt).

0009-2541/02/$ - see front matter © 2002 Elsevier Science B.V. All rights reserved.
PII: S0009-2541(02)00135-3

where c is the concentration of sodium in the solution and c_{eq} its equilibrium concentration with respect to halite. The quantity k is a rate constant in mol cm^{-2} s^{-1}, and the concentrations are in mol/cm^3. Rate equations have also been expressed in terms of the ion-activity product (IAP) by

$$R = k\left(1 - \frac{\mathrm{IAP}}{K_c}\right) \tag{2}$$

where K_c is the solubility product of the corresponding mineral.

For many minerals, such simple rate equations are not adequate and a more complex equation must be used. A common empirical rate equation is

$$R = k_n\left[1 - \frac{c}{c_{eq}}\right]^n \tag{3}$$

where, $n \neq 1$, is an empirical reaction order (Lasaga, 1998). Such nonlinear rate equations indicate a complex interplay of transport and chemical processes at the surface of the mineral. In studies of the dissolution kinetics of calcite in seawater rate equations in the form

$$R = k\left(1 - \frac{(Ca^{2+})(CO_3^{2-})}{K_c'}\right)^n \tag{4}$$

have commonly been reported. K_c' is the stochiometric solubility product of calcite in seawater. In a detailed laboratory work for calcite in seawater, Keir (1980) found $n = 4.5$, and $K_c' = 4.8 \times 10^{-7}$ mol^2 kg^{-2}.

More complicated rate equations have been found for natural calcite minerals, e.g. Iceland spar (Plummer and Wigley, 1976; Plummer et al., 1978; Palmer, 1991) and limestone (Svensson and Dreybrodt, 1992; Eisenlohr et al., 1999), and also for natural gypsum (Jeschke et al., 2001) These rate equations show a switch from order n_1 to order n_2 by

$$\begin{aligned} R_1 &= k_{n_1}\left(1 - \frac{c}{c_{eq}}\right)^{n_1} \quad \text{for } c \le c_s \\ R_2 &= k_{n_2}\left(1 - \frac{c}{c_{eq}}\right)^{n_2} \quad \text{for } c > c_s \end{aligned} \tag{5}$$

where c is the calcium concentration in the solution, c_{eq} the corresponding equilibrium concentration, and c_s, the concentration where the kinetics switch to higher order. c_s is between 0.7 and $0.9c_{eq}$ for limestone, and about $0.95c_{eq}$ for gypsum.

To find the rate constants k and n from experimentally determined rates one must use a fitting procedure. The most simple one is to plot $\log(R)$ versus $\log(1 - c/c_{eq})$. Rate equations such as in Eqs. (1)–(4) will then plot as straight lines,

$$\log(R) = n\log\left(1 - \frac{c}{c_{eq}}\right) + \log(k) \tag{6}$$

from the slope of which one can read n. $\log(k)$ can be read from the point of intersection of the curve with the $\log(R)$ axis at $c = 0$. For rate equations such as Eq. (5), the same procedure reveals two segments of straight lines, with slopes n_1 and n_2. $\log(k_{n_1})$ and $\log(k_{n_2})$ can be found by extrapolation to $c = 0$. This method, however, has to be applied with extreme care, because the result depends critically on the value of c_{eq} that one uses.

Hales and Emerson (1997) re-examined seawater dissolution rates from Keir (1980). Using the most recent data for $K_c' \approx 3.9 \times 10^{-7}$ mol^2 kg^{-2}, which is lower by about 20% compared to that used by Keir, who proposed a nonlinear rate law, they claimed an entirely linear rate equation. Employing this rate equation, in situ measurements of pore waters on calcite-rich sea floor sediments could be explained more consistently than by applying Keir's equation.

In the present article, we will elaborate a method to determine the kinetic parameters n, k, and c_{eq} from experimental data and to show the pitfalls, which can lead to wrong conclusions.

2. Theory and method

In the following, we will demonstrate the pitfalls arising by using incorrect values of c_{eq} in the evaluation of experimental data and we suggest a systematic numerical procedure to avoid them. To this end, we construct a set of virtual experimental data from a known rate equation. By this way, we obtain data which relates the rates to the chemical composition x of the solution. We truncate this set to some final value $x_f < x_{eq}$, where, e.g. a free drift experiment has been terminated. Such a set of virtual data is equivalent to a real set of experimental data. We can

demonstrate the validity of our method, if we can recover the rate law, known in the case of virtual data, by use of the truncated virtual data exclusively without any further information. We first deal with a rate equation given by

$$R = k\left(1 - \frac{x}{x_{eq}}\right)^n \tag{7}$$

In Eq. (7), x stands for c or IAP, respectively, and x_{eq} is the corresponding true equilibrium value. In the following, we will call this a homogeneous equation.

From the truncated data set, we only know that $x_{eq} > x_f$. When plotting the rates versus $(1 - x/x_{eq})$ in a double logarithmic plot, we therefore have to estimate some value x_0 which could deviate from x_{eq} by Δx; $x_0 = x_{eq} + \Delta x$. The rates which one finds by plotting the data using x_0 instead of x_{eq} are shown by Fig. 1.

The full straight line presents Eq. (7) with true x_{eq}, or in other words $\Delta x = 0$. The dashed lines above this curve are obtained, when $\Delta x = -0.1x_{eq}$ or $-0.01x_{eq}$, respectively. Note that for each of the curves the corresponding value of Δx is used in $\log[1 - x/(x_{eq} + \Delta x)]$. Therefore with respect to x, each curve has a different scale on the abscissa. The upper curves represent the case, when $x_0 < x_{eq}$. It may also happen that for some reasons, the estimated value of x_0 could be above x_{eq}. This case is shown by the lower set of curves, where $\Delta x = +0.1x_{eq}$ or $+0.01x_{eq}$, respectively.

In all cases, there is good agreement to the correct plot with $x_0 = x_{eq}$ for x close to zero. The range of agreement depends on Δx. Considering that most data in dissolution experiments are obtained below $x = 0.99x_{eq}$ ($\log[1 - x/x_{eq}] = -2.0$), one envisages from Fig. 1 that plotting the rates with $\Delta x \neq 0$ leads to curves, which easily could be misinterpreted as a change of the order of the kinetics.

In Fig. 2a, we have replotted the upmost curve of Fig. 1 with $\Delta x = -0.1x_{eq}$, and in Fig. 2b the lowest curve with $\Delta x = +0.1x_{eq}$ is depicted. Such curves will likely be obtained from plots of experimental data where $x_0 = x_{eq} + \Delta x$ has been taken for true equilibrium erroneously. The aim is now to find from such a plot the true value of x_{eq} and the correct values of k and n, provided the rate equation follows Eq. (7).

Let us assume that experimental data has been obtained from a mineral with a homogeneous non-

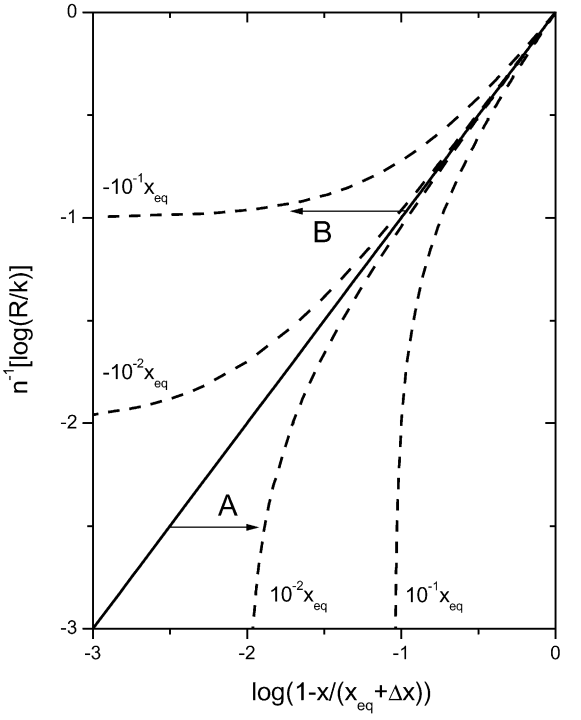

Fig. 1. Various double logarithmic plots of a rate equation $R = k(1 - x/x_{eq})^n$. The full line depicts the plot of rates versus $\log(1 - x/x_{eq})$. The dotted lines present plots of the rates versus $\log[1 - x/(x_{eq} + \Delta x)]$. The value of Δx is given by the numbers on the curves. Note that by plotting the rates to this new scale, each point from the full line is shifted parallel to the abscissa to the point on the corresponding curve. This is illustrated by arrows A and B.

linear kinetics as described by Eq. (7). These are given by data points which relate the rate R to the chemical composition x of the solution. To find out whether these can be described by Eq. (7) in a first step $\log(R)$ is plotted versus $\log(1 - x/x_0)$, where x_0 is a first guess of x_{eq}. Fig. 2 shows a plot of such data for $x_0 = 0.9x_{eq}$ (a), and $x_0 = 1.1x_{eq}$ (b). From such curves x_{eq} must be determined, such that a plot of $\log(R)$ versus $\log(1 - x/x_{eq})$ plots as a straight line from which k and n can be determined. If the rates obey Eq. (7), this is trivial. One just has to vary x_0 until a straight line is obtained which coincides with all data points.

The problem arises for minerals exhibiting an inhomogeneous kinetics as given by Eq. (5), with a switch from order n_1 to n_2 at a switch value x_s. A few comments should be given first at that point: (1) The experimentally observed switch is not sudden as

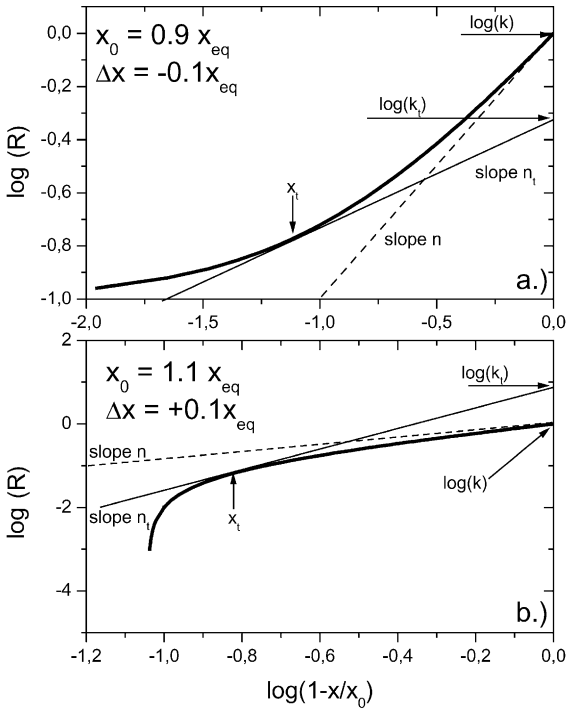

Fig. 2. Plot of log(R) versus an erroneous value x_0, which deviates from x_{eq}. (a) $x_0 = 0.9x_{eq}$, (b) $x_0 = 1.1x_{eq}$. The tangent drawn to the curve at x_t has slope n_t and the value log(k_t) is given by its intersection with the ordinate at $\log(1 - x/x_0) = 0$. The dotted line depicts the tangent to the curve at $x_t = 0$. log(k) and n can be read from it.

assumed in our idealized equations, but is steady from n_1 to n_2 in narrow region as can be visualised from the experimental data of Jura limestone in Fig. 5. The transition region, however, is sufficiently small, to allow the mathematical idealisation. As a consequence, the experimental data cannot be perfectly fitted in this narrow region. (2) The aim of our procedure is not to reveal the mechanistic processes which cause the nonlinear kinetics, but rather to find a reliable way to extract a correct empirical rate equation, by which n, k, and c_{eq} can be obtained. Now plotting log(R) versus $\log(1 - x/x_{eq})$, one obtains a curve as given by the full line in Fig. 3. One does not know then from the experimental data whether the change of slope is caused by a wrong estimation of x_{eq} or by the inhomogeneous kinetics of the mineral. In the case of inhomogeneous kinetics, simply varying x_{eq} will not suffice. Therefore, we must divide the data set into two sections. The first covers the region below x_s and the second one above x_s, whereby x_s can only crudely be estimated. Both data sets are incomplete since they do not cover the entire region of x-values.

To find out whether such an incomplete set can be described by a nonlinear rate equation, we use the following systematic procedure. We turn back to Fig. 2 where we have presented plots with $x = 0.9x_{eq}$ and

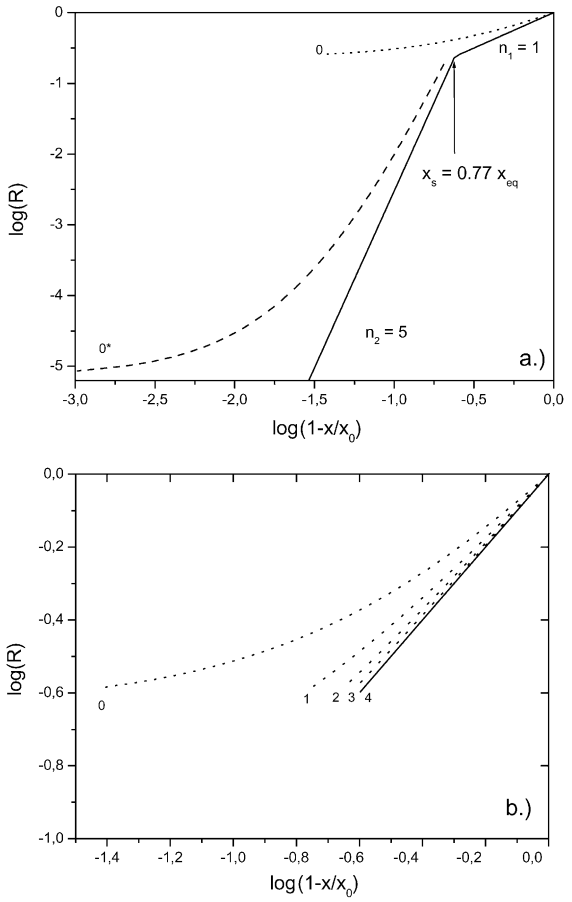

Fig. 3. (a) Plot of an inhomogeneous rate equation (cf. Eq. (5)) with $n_1 = 1$ and $n_2 = 5$, $x_s = 0.77x_{eq}$ with curves for various values of x_0. See text. The full line is for $x_0 = x_{eq}$ and represents the correct plot. Curve 0 is a plot with $x_0 = 0.77x_{eq}$ (using only data $x < x_s$), and curve 0* results by using $x_0 = 0.97x_{eq}$ (for the data $x > x_s$). (b) Magnified plot of the upper right-hand side corner of (a). Curves 1, 2, 3, and 4 result from the iterative procedure with values of x_0 as depicted by the arrows in Fig. 4a.

$x_0 = 1.1x_{eq}$. We select an arbitrary point with x_t on that curve and draw a tangent to it. Then the rate at x_t can be written as

$$R_t = k_t\left(1 - \frac{x_t}{x_0}\right)^{n_t} \tag{8}$$

where n_t is the slope of the tangent in the double logarithmic plot of Fig. 2, and $\log(k_t)$ can be read from the point of intersection of the tangent with the $\log(R)$-axis at $\log(1 - x/x_0) = 0$.

On the other hand, for the point x_t the true rate equation

$$R = k\left(1 - \frac{x_t}{x_{eq}}\right)^{n} \tag{9}$$

is also valid. By equating Eqs. (8) and (9), one obtains for each point x_t.

$$x_{eq} = \frac{x_t}{1 - \left(\frac{k_t}{k}\right)^{\frac{1}{n}}\left(1 - \frac{x_t}{x_0}\right)^{\frac{n_t}{n}}} \tag{10}$$

In this equation, n_t, k_t, x_t, and x_0 are known. The parameters n and k must be estimated from the tangent to the (virtual) experimental points at $x_t = 0$. If data points are not available there, as is the case for the data set with $x > x_s$ (part n_2), n and k must be estimated to a lower degree of accuracy from the tangent to the data points with lowest x available. In any case, k and n are first estimations only and consequently only a first approximation $x_{eq}^{(1)}$ can be obtained from Eq. (10).

If $x_0 \neq x_{eq}$ then n_t and k_t are functions of x_t and $x_{eq}^{(1)}$ is a function of x_t. On the other hand, if $x_0 = x_{eq}$ the plot will be a straight line with $n_t = n$ and $k_t = k$ everywhere and consequently $x_{eq}^{(1)} = x_{eq}$ is independent of x_t.

We use this fact to find x_{eq} by an iterative procedure. We start to plot the data with some first approximation x_0 and calculate $x_{eq}^{(1)}$ from Eq. (10). If it exhibits a functional dependence on x_t, we use the maximum or minimum value $x_{eq}^{m} = x_0$ for the next plot. From this, we calculate $x_{eq}^{(2)}$ by use of Eq. (10). Employing the result, which shows the lowest functional variation in dependence on x_t. We repeat this procedure, until the variation of $x_{eq}^{(i)}$ stays within a limit Δx_{eq}. The final average value of $x_{eq}^{(final)}(x_t) \pm \Delta x_{eq}$ then gives a satisfactory value for x_{eq}.

We demonstrate this procedure in what follows. In Fig. 3a, we have plotted a hypothetical inhomogeneous rate equation with $n_1 = 1$, $n_2 = 5$ and $x_s = 0.77x_{eq}$. The full line shows the correct plot to the rate equation, with $x_0 = x_{eq}$, with two sections: one with slope $n_1 = 1$ and the other with steeper slope $n_2 = 5$ for $x > x_s$.

What could have been found by an experimentalist is shown by curves 0* and 0, which have been obtained by plotting the experimental data using $x_0 = 0.97x_{eq}$ (curve 0*) or $x_0 = 0.77x_{eq}$ (curve 0). From curve 0, first estimations of n and k can be obtained drawing the tangent to the curve at the lowest values of x_t available. These values are used as n and k in Eq. (10) for $x < x_s$ to obtain $x_{eq}^{(1)}$ shown by Fig. 4a, curve 1. Clearly, $x_{eq}^{(1)}$ is a function of x_t and does not fulfil the requirement of independence of x_t. We now use the largest value of $x_{eq}^{(1)} = 0.9x_{eq}$, at $x_t = 0.77x_{eq}$ (curve 1 in Fig. 4a) as a new value $x_{eq}^{(1)}$ to plot the rate equation with $(1 - x/x_{eq}^{(1)})$. The result is given by the dotted curve 1 in Fig. 3b. Using this curve to estimate n and k and iteratively applying Eq. (10), we obtain a second iteration $x_{eq}^{(2)}$ which is shown by curve 2 in Fig. 3b. Repeating this procedure, we find iteratively curves 2, 3, 4 in Fig. 3b, and corresponding curves 2, 3, and 4 for $x_{eq}^{(n)}$ in Fig. 4a. Although the initial guess of x_0 deviates by 23% from the true value, our procedure reveals the true value of $x_{eq} = 1$ after only four iterations, and the resulting curve 5 fits perfectly to the true plot of the rate equation. Note that by employing this procedure we have also obtained the values k and n iteratively.

We now turn to the remaining points in Fig. 3a covering the region with order n_2, i.e. $x > 0.77x_{eq}$. The last point of the true curve in Fig. 3a is at $x = 0.97x_{eq}$. We could take this as a first approximation for x_0. Curve 0* in Fig. 3a shows the plot with $x_0 = 0.97x_{eq}$. Estimating n and k from the experimental data close to x_s and using the above value of $x_0 = 0.97x_{eq}$ to estimate $x_{eq}^{(1*)}$, we find curve 1* depicted in Fig. 4b. There is only a slight dependence of $x_{eq}^{(1*)}$ on x_t, such that $x_{eq}^{(1*)} = x_{eq} \pm 0.005x_{eq}$. Plotting the data of curve 0* with this value of x_0 yields a curve which coincides with the curve of the true rate equation. These examples show that the iterative fitting procedure is

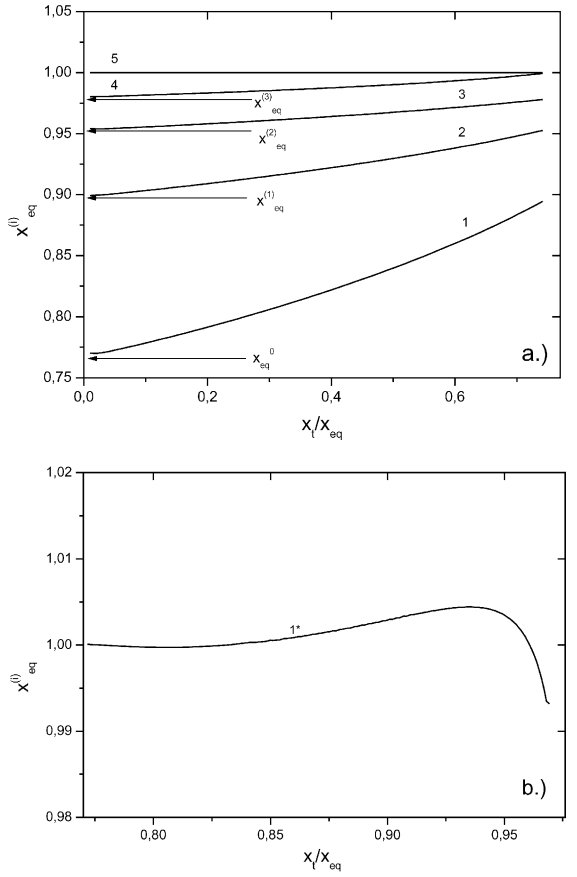

Fig. 4. (a) Values of $x^{(i)}_{eq}$ as a function of x_t for the iterative procedure to recover the true plot from curve 0 of Fig. 3b. (b) The first iterative step to recover true x_{eq} from curve 0* in Fig. 3a. After only one iteration, true x_{eq} is found with an accuracy of $\pm 0.5\%$. Plotting curve 0* with this value gives satisfactory agreement with the correct plot. Note that we plot x_t/x_{eq} in the abscissa.

a suitable tool to recover the rate equation and the values of the corresponding parameters. If minerals show rate equations according to Eqs. (1)–(5), our method enables us to find the true value of c_{eq} or K_c from first crude estimations of about 10% accuracy. It should be pointed out here that c_{eq} obtained from the region with n_1, and c_{eq} obtained from the region with n_2 are determined independently. Only if these two values coincide within the limits of error the fitting procedure can be regarded as reliable, and describes correctly all experimental values far and close to equilibrium.

3. Application to limestone

In the following, we will discuss the application of the iterative procedure to real experimental data obtained from calcium carbonate minerals. Fig. 5 shows a plot of such experimental data obtained in our laboratory by employing a free drift batch experiment on Jura limestone under conditions closed with respect to CO_2 in an aqueous solution with an initial CO_2-pressure of 0.05 atm at a temperature of $T=10$ °C. Dissolution for pure limestone, such as used proceeds stoichiometrically and carbonate concentrations can be obtained by use of PHREEQC (Parkhurst and Appelo, 1999) from initial p_{CO_2} and Ca-concentration in the solution. Details of such an experimental set-up are reported by Eisenlohr et al. (1999). Plotting the experimental points, the value $c_0=2.3$ mmol/l was used. The resulting curve shows a switch from order $n_1=1.1$ to $n_2=3.4$. To verify this as a valid rate equation, we use the method described in the previous chapter.

We first investigate the n_1-part of the data. Plotting this data using $c_0=1.82$ mmol/l one gets curve 0.

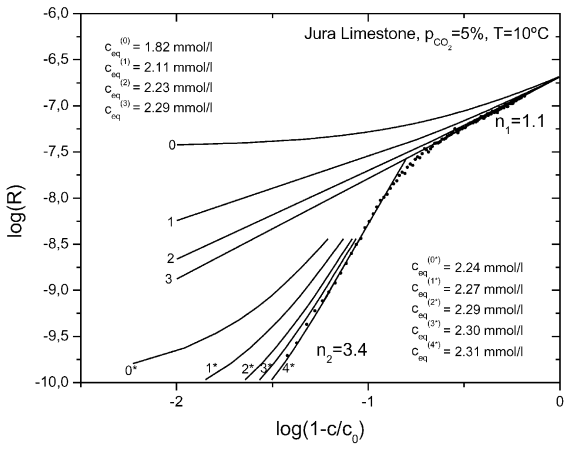

Fig. 5. Dissolution rates of limestone: The points depict the experimental data plotted versus the correct $c_{eq}=2.30$ mmol/l. Plotting with $c^{(0)}_{eq}=1.82$ mmol/l would put these points on curve 0. The numbers on the upper left corner depict the values of $c^{(i)}_{eq}$. The corresponding curves are plots using the respective values. Curve 3 fits to the correct plot with $c^{(3)}_{eq}=2.29$ mmol/l. Using an initial $c_0^*=2.24$ mmol/l would put the experimental points to curve 0*. The values of $c^{(i)}_{eq}$* on the lower right corner depict the values of $c^{(i)}_{eq}$* from the iterative procedure. Curve 4* coincides with the correct plot. Note that curves 1, 2, and 3 have been extended beyond the region of the available data points for better visualisation.

From this curve, we now recover the true rate equation. The iterative procedure using this data points yields as a first approximation the $c_{eq}^{(1)}$-curve 1 in Fig. 6a. Using the maximal value of $c_{eq}^{(1)}$ as a first approximation, we obtain curve 1 in Fig. 5. Further iterations yield curves 2 and 3 in Figs. 5 and 6a, respectively. The curves show some "noise" since experimental data has been used. The final rate equation from curve 3 yields $n_1 = 1.1$, $k_1 = 2.1 \times 10^{-7}$ mmol cm^{-2} s^{-1} and $c_{eq} = 2.29 \pm 0.006$ mmol/l. (Note that curves 1,2, and 3 have been extended beyond the region of the available data points for better visualisation.)

We now turn to the part with higher slope n_2. The experiment has been terminated at $c_{end} = 2.24$ mmol/l. Starting the iterative procedure with this value, one obtains curves 0*, and by iteration the curves 1*, 2*, 3* and 4* in Figs. 5 and 6b, respectively. From this, we find $c_{eq}^{(4)} = 2.315 \pm 0.005$ mmol/l. As one has to expect, both values of c_{eq} obtained from the two regions are close together. Using a final average value $c_{eq} = 2.30 \pm 0.01$ mmol/l, one obtains a reliable rate equation. From this, we find $n_1 = 1.1$, $n_2 = 3.4$, $k_1 = 2.1 \times 10^{-7}$ mmol cm^{-2} s^{-1}, $k_2 = 1.1 \times 10^{-5}$ mmol cm^{-2} s^{-1}. The rate equation with these values is also plotted by the curves 3 and 4* in Fig. 5. It fits well to the experimental data, except in a region close to the switch concentration. Therefore, within the limit of accuracy, the procedure assures that a switch of the kinetic order is correct. This switch is characteristic for natural calcite-minerals and has also been observed in experiments with natural gypsum (Jeschke et al., 2001).

Batch experiments on synthetic calcite, however, reveal an almost linear rate equation, according to theoretical predictions (Dreybrodt et al., 1996; Svensson and Dreybrodt, 1992). We have also evaluated this experimental data. Fig. 7 shows the experimental points of a free drift batch experiment plotted with $c_0 = 2.13$ mmol/l. As in the previous case, we assume that the experiment has been terminated at lower concentration of $c_{eq}^{(0)} = 1.72$ mmol/l. A plot using this value is depicted by curve 0 in Fig. 7a. Now again using the iterative procedure, we obtain from curve 0 in Fig. 7a and curve 1 in Fig. 7b which depicts a new $c_{eq}^{(1)}$. After seven iterations, we obtain curve 7 with $c_{eq}^{(7)} = 2.13$ mmol/l in Fig. 7b from which we obtained curve 7 in Fig. 7a. It fits well to the experimental points and reveals a rate equation with $n = 0.8$ and $k = 2.5 \times 10^{-7}$ mmol cm^{-2} s^{-1}. This rate equation is in close agreement to theoretical calculations, which have considered the empirical equations of Plummer et al. (1978) and the slow conversion of CO_2 into $H\dot{C}$

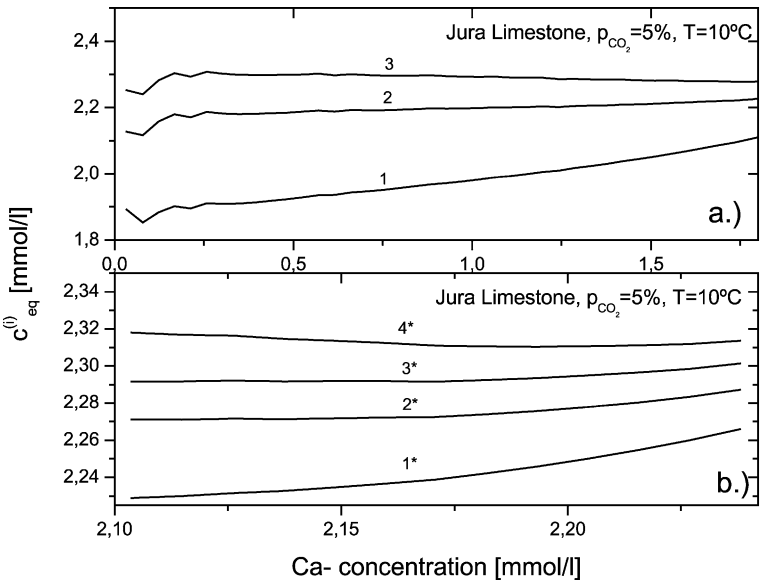

Fig. 6. (a) Values of c_{eq}^{i} for the n_1-part of Fig. 5 as a function of c. (b) Values of $c_{eq}^{(i)}$* for the n_2-part of Fig. 5 as a function of c.

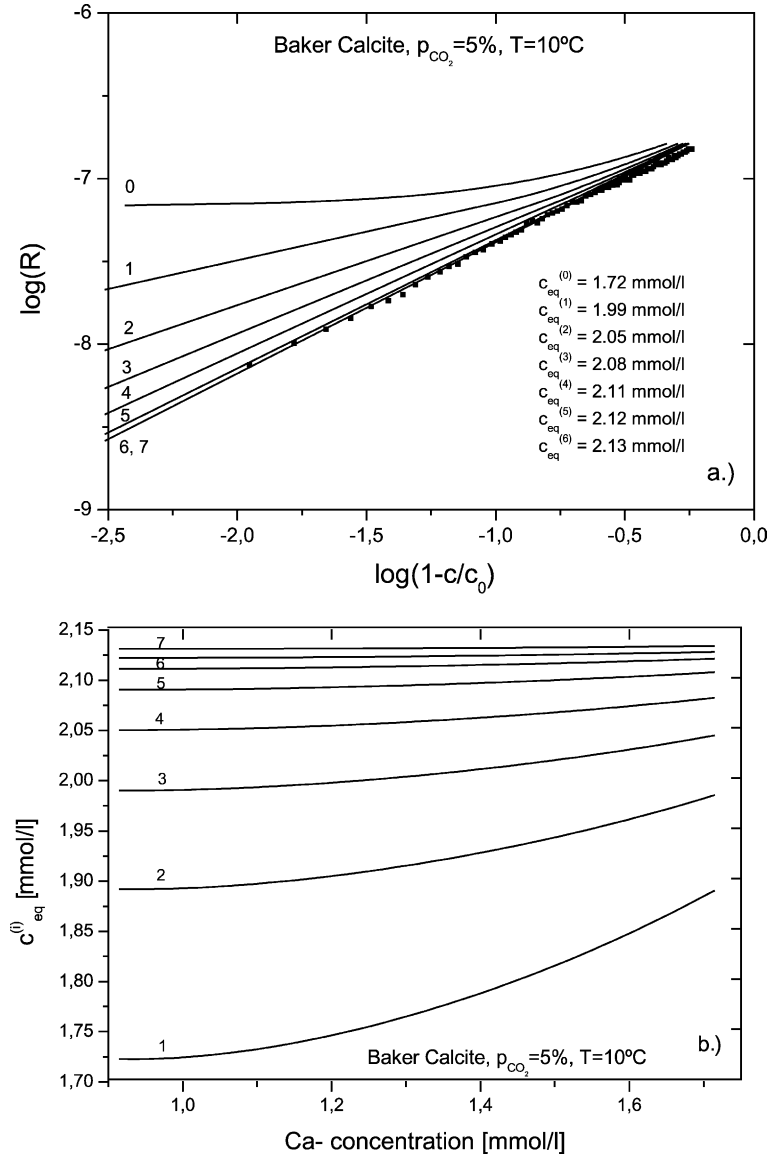

Fig. 7. Dissolution rates of synthetic calcite: (a) Iterative procedure. Meaning of $c_{eq}^{(i)}$ and curves 0 to 7 is analogous to Figs. 5 and 6. (b) The values of $c_{eq}^{(i)}$ used in (a) as function of c.

and HCO_3^- (Dreybrodt et al., 1996; Buhmann and Dreybrodt, 1985a,b). It should be noted at this point that the equilibrium value $c_{eq}=2.13$ mmol/l is in close agreement to calculations performed with PHREEQC (Parkhurst and Appelo, 1999). For natural Jura limestone, a somewhat higher value $c_{eq}=2.30$ mmol/l is obtained. This is due to a concentration of 3.1 mol% of Mg in the solid (Eisenlohr et al., 1999) which changes the solubility product (Appelo and Postma, 1999).

It should be pointed out that gypsum also exhibits inhomogeneous nonlinear rate equations. We revised the data given by Jeschke et al. (2001) by use of our method and have found them to be valid. The results are not presented here because they are analogous to those of limestone.

4. Application to anhydrite

Anhydrite ($CaSO_4$) plays an important role in the evolution of gypsum karst (Klimchouk et al., 1996). Furthermore, dissolution of anhydrite contributes to geohazard in the vicinity of hydraulic structures, such as damsites, or upon extraction of groundwater (James, 1992; Cooper, 1986). The knowledge of its dissolution kinetics is therefore highly relevant.

The equilibrium concentration of Ca with respect to anhydrite is 22.9 mmol/l at 10 °C, higher than that with respect to gypsum at 14.44 mmol/l. These values have been found employing the program PHREEQC (Parkhurst and Appelo, 1999) with the database PHREEQC.dat. Therefore, reliable measurements of the dissolution kinetics of anhydrite can only be performed for concentrations below saturation with respect to gypsum. For concentrations above this value gypsum precipitation is likely. Although in free drift batch experiments higher concentrations are obtained until precipitation starts, one cannot be sure that gypsum does not precipitate from the supersaturated solution. If this is the case, the dissolution rates for anhydrite measured in such an experiment are no longer reliable. Therefore, only a limited experimental data set with $c < 0.62 c_{eq}^{anh}$ is available, from which one has to recover the rate equation. This may be the reason, why up to now little is known on the dissolution kinetics of anhydrite.

We have performed free drift batch experiments on anhydrite at 10 °C, using anhydrite particles of about 565 μm diameter. The anhydrite samples contained 0.85 wt.% MgO and some trace elements below 0.1 wt.%. In a free drift experiment for such pure minerals dissolution is stoichiometrical and SO_4 can be calculated from the Ca-concentration in the solution. Details of the experimental set-up and the methods are given elsewhere (Jeschke et al., 2001). The experimental conditions are such that dissolution is controlled by surface reactions and that transport control does not limit the rates. Details will be reported elsewhere. In this context, we only give the basic results. The particles were obtained from a piece of natural anhydrite taken from a bore core of anhydrite rock from Sangershausen, Harz, Germany. The sample was analysed by X-ray fluorescence. It contained 0.85 wt.% Mg and 1500 ppm Sr. The sample was heated at 300 °C until no further weight loss occurred. Maximal weight loss detected was about 1 ‰ of the weight, showing that the sample is pure anhydrite.

Fig. 8a shows the time dependence of the calcium concentration for a free drift batch experiment. After a steep rise, the concentration increases slowly reaching a value well above the equilibrium concentration of gypsum and then decreases as gypsum is precipitated. Finally when anhydrite dissolution and precipitation of gypsum balance a stationary value will be obtained. Only the data below c_{eq} with respect to gypsum is

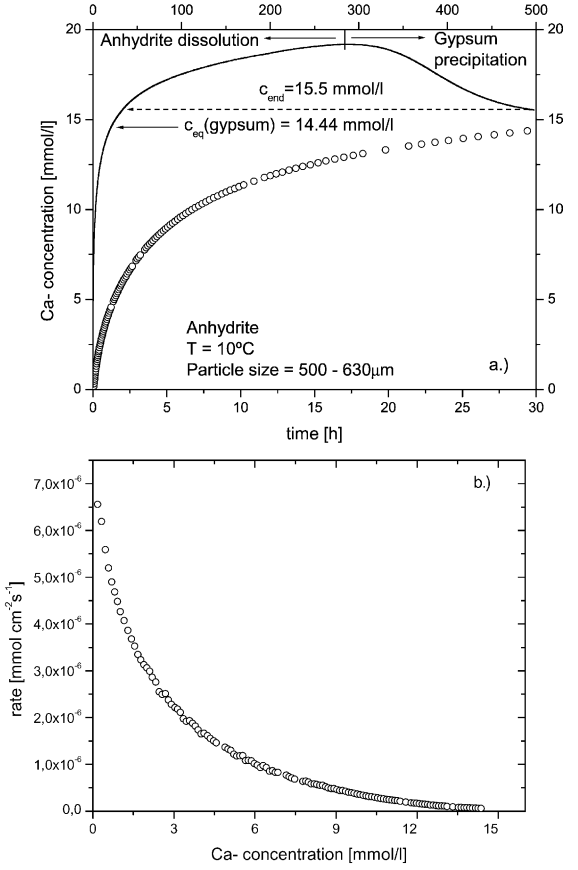

Fig. 8. Dissolution of anhydrite: (a) Calcium concentration in dependence on time (upper scale) obtained in a free drift batch experiment. The full line depicts the entire evolution of Ca-concentration of anhydrite. Precipitation of gypsum is seen from the declining concentration. The open circles show the experimental data points obtained for concentrations below the equilibrium concentration with respect to gypsum during the first 30 h (lower time scale). (b) Rates as a function of the calcium concentration obtained from the data points of (a).

reliable to obtain dissolution rates. From this curve, the rates are calculated by

$$R = \frac{V}{A}\frac{\mathrm{d}c}{\mathrm{d}t} \tag{11}$$

where V is the volume of the solution and A the surface area of the mineral it has been estimated from the geometry of the particles. Fig. 8b shows the rates as obtained by Eq. (11) as a function of concentration. We have also performed experiments on anhydrite by use of the rotating disk set up, as described by Jeschke et al. (2001). Rates obtained from such experiments by using the geometric area of the disk, compare reasonably well to those obtained from the batch experiment within 40%. This justifies the use of the geometrical surface area in the batch experiments. Fig. 9a, curve 0, shows a logarithmic plot of the experimental rate data for concentrations of Ca below 14.44 mmol/l plotted against $c_0 = 22.0$ mmol/l. Starting with this value, we employ the iteration procedure. Fig. 9b depicts the curves of $c_{\mathrm{eq}}^{(i)}$, $i = 1-4$. After four iterations, $c_{\mathrm{eq}}^{(4)}$ becomes almost independent on c. Using this value, $c_{\mathrm{eq}}^{(4)} = 23.5 \pm 0.1$ mmol/l, one finds curve 4 in Fig. 9a, where also the experimental data points are plotted. Therefore, we conclude that in the region where experimental data is available a nonlinear rate equation is valid, with $n = 4.5 \pm 0.2$ and $k = 5.0 \pm 1 \times 10^{-6}$ mmol cm^{-2} s^{-1}. It should be pointed out that by simply using logarithmic plots it would not be possible to decide whether curve 0 or curve 4 is correct, because due to the incomplete data set both plot as straight lines in that regions. As a further confirmation of our method, we have measured dissolution rates of anhydrite for $T = 5$ °C. Due to the lower temperature, this solution has a lower equilibrium concentration of 21.96 mmol/l, calculated with PHREEQC. From the experimental data, we find a rate equation with $c_{\mathrm{eq}} = 21.4 \pm 0.2$ mmol/l, $k = 3.2 \pm 0.8 \times 10^{-6}$ mmol cm^{-2} s^{-1} and $n = 4.8 \pm 0.2$. Details about the dissolution kinetics of anhydrite in dependence on temperature and concentration of sodium chloride will be presented in a separate paper.

Just one comment should be given. Our findings are in contrast to the results of James and Lupton (1978) and James (1992) who reported a second-order rate equation ($n = 2$). One has to consider, however, that the experimental set-up employed in their work does not provide surface controlled rates. Instead, the

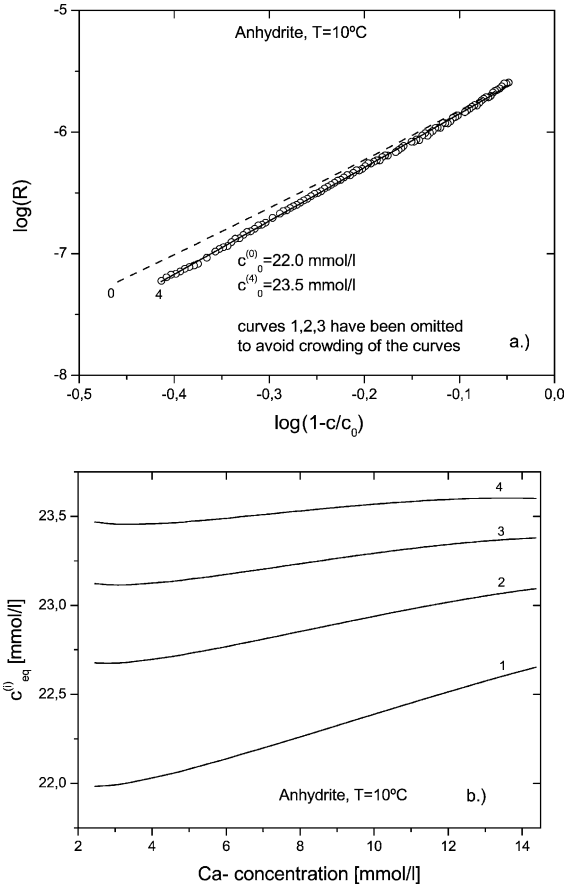

Fig. 9. (a) Iterative procedure to find the rate equation for anhydrite from experimental data of the free drift batch experiment. (b) The iterative values of $c_{\mathrm{eq}}^{(i)}$ for the anhydrite data from (a). The final equilibrium value $c_{\mathrm{eq}}^{(4)} = 23.5 \pm 0.1$ mmol/l is close to the theoretical value.

experimental data reveal that transport control is involved. In such a case of mixed kinetics one cannot find, without further information, the surface controlled rate equation (Jeschke et al., 2001). We have calculated the effective rates using the surface-controlled rate equation for anhydrite as described above and a linear transport equation $R_t = k_t(1 - c/c_{\mathrm{eq}})$. If one assumes $k_t = 0.37k_s$, the effective rates show a second-order rate equation, fitting well to the experimental data of James and Lupton. This reconciles the apparent contradiction.

Our experimental data give also some hints on the mechanism of the anhydrite-gypsum conversion. The

initial dissolution rates of anhydrite measured in this experiment are by about two orders of magnitude smaller than those of gypsum measured in the same experimental set up (Jeschke et al., 2001). If anhydrite would convert to gypsum by uptake of H_2O-molecules into the lattice then the gypsum originating at the surface of the particles would be removed immediately by dissolution. Thus, at lower concentrations, one would expect a sum of two rates: (a) dissolution of anhydrite and (b) a constant additional dissolution rate of the gypsum converted from anhydrite by direct uptake of water molecules. It is extremely unlikely that this complicated mechanism can be described by a single rate equation using solely the correct value of c_{eq} with respect to anhydrite. Anhydrite-gypsum conversion by direct uptake of water at least must be very slow. Under our experimental conditions, anhydrite-gypsum conversion is driven by dissolution of anhydrite until a supersaturated solution with respect to gypsum is reached, and gypsum is precipitated subsequently.

5. Conclusion

Dissolution rates of some minerals in aqueous solutions obey either a linear rate equation $R = k_1(1 - c/c_{eq})$ or a nonlinear one, $R = k_n(1 - c/c_{eq})^n$. To find k and n reliably from a double logarithmic plot of R against $(1 - c/c_{eq})$, the value of c_{eq} must be known to a high degree of accuracy. Small deviations from true c_{eq} could mimic a change of the order n in the empirical rate equation. In most experiments, the data close to equilibrium is incomplete such that c_{eq} cannot be determined with sufficient accuracy. We have presented a method to find reliable values of c_{eq}, k, and n from such incomplete data sets.

Some minerals, however, close to equilibrium, exhibit a switch from linear to nonlinear kinetics, e.g. limestone and gypsum rocks. To establish such rate equations, we suggest a fitting procedure to the experimental data of free drift dissolution experiments, from which k, n, and c_{eq} can be obtained. This is of high significance since in most natural conditions, e.g. natural minerals, due to impurities in the solid and aqueous phases, c_{eq} deviates slightly from what one obtains by using thermodynamical data of the idealized pure $CaCO_3$–H_2O–CO_2 system. Therefore, especially close to equilibrium the rate equations must be determined with extreme care. Using values of c_{eq} deviating only slightly from the true values yields unreliable results, especially close to equilibrium where many geochemical processes are operative.

This work here does not aim to elucidate the physics and chemistry of the detachment mechanism of ions from the mineral, but has the purpose to obtain a reliable tool to find an empirical rate equation, which depends on easily accessible parameters, such as Ca-concentration in the solution. This is of relevance as different limestones show values of n in the range between 3 and 8 (Eisenlohr et al., 1999). Therefore, for geological purposes at specific sites, measurements of rate equations of the rocks are of importance, and a reliable tool to evaluate the results is needed.

Simple empirical rate equations are of high relevance for modelling dissolution of limestone or gypsum to understand the evolution of karst aquifers under natural conditions, and under their changes by the construction of damsites in terrains of these soluble rocks (James, 1992; Dreybrodt, 1996; Dreybrodt et al., 2002).

Furthermore, natural minerals differ from synthetic pure compounds by incorporation of trace metals and phosphate which give rise to inhibition of dissolution. The reaction order n in these materials is an empirical parameter and does not have a clear-cut interpretation since many different mechanisms contribute. The rate equations discussed here have been obtained in free drift experiments and therefore can be applied to many geological situations.

On the other hand, the empirical rate equations can be converted to functions depending on the relevant ion activity products. In all experimental cases discussed here, it is straightforward to calculate the ionic activity product by use of equilibrium programs, such as PHREEQC, from the Ca-concentration for gypsum and anhydrite. For calcite, additional knowledge of p_{CO_2} of the solution is necessary. By this way, measurements of rates in their dependence of Ca-concentration may help to find rate laws, which reflect the mechanistic principles of dissolution and its inhibition in natural materials close to equilibrium. This could be a perspective for further work.

Acknowledgements

One of us, A.J. thanks the "Stiftung Constantia v. 1823, Bremen" for financial support. We would like to express thanks to Dr. Oelkers, Dr. Wogelius and an anonymous reviewer for their comments, which helped to improve the paper. **[EO]**

References

Alkattan, M., Oelkers, E.H., Dandurand, J.-L., Schott, J., 1997. Experimental studies of halite dissolution kinetics: 1. The effect of saturation state and the presence of trace metals. Chem. Geol. 137, 201–219.

Appelo, C.A.J., Postma, D., 1999. Geochemistry, Groundwater and Pollution, 3rd ed. A.A. Balkema, Rotterdam.

Buhmann, D., Dreybrodt, W., 1985a. The kinetics of calcite dissolution and precipitation in geologically relevant situations of karst areas: 1. Open system. Chem. Geol. 48, 189–211.

Buhmann, D., Dreybrodt, W., 1985b. The kinetics of calcite dissolution and precipitation in geologically relevant situations of karst areas: 2. Closed system. Chem. Geol. 53, 109–124.

Cooper, A.H., 1986. Subsidence and foundering of strata causes by the dissolution of Permian gypsum in the Ripon and Bedale areas, North Yorkshire. In: Harwood, G.M., Smith, D.B. (Eds.), The English Zechstein and Related Topics. Geological Society Special Publication, vol. 22, pp. 127–139.

Dreybrodt, W., 1996. Principles of early development of karst conduits under natural and man-made conditions by mathematical analysis of numerical models. Water Resour. Res. 32, 2923–2935.

Dreybrodt, W., Laukner, J., Liu, Z., Svensson, U., Buhmann, B., 1996. The kinetics of reaction $CO_2 + H_2O \rightarrow H^+ + HCO_3^-$ as one of the rate limiting steps for the dissolution of calcite in the system $H_2O-CO_2-CaCO_3$. Geochim. Cosmochim. Acta 60, 3375–3381.

Dreybrodt, W., Romanov, D., Gabrovšek, F., 2002. Karstification below dam sites: a model of increasing leakage from reservoirs. Environ. Geol. Published online DOI 10.1007/s00254-001-0514-7.

Eisenlohr, L., Meteva, K., Gabrovšek, F., Dreybrodt, W., 1999. The inhibiting action of intrinsic impurities in natural calcium carbonate minerals to their dissolution kinetics in aqueous H_2O-CO_2 solutions. Geochim. Cosmochim. Acta 63, 989–1002.

Hales, B., Emerson, S., 1997. Evidence in support of first-order dissolution kinetics of calcite in seawater. Earth Planet. Sci. Lett. 148, 317–327.

James, A.N., 1992. Soluble Materials in Civil Engineering. Ellis Horwood, Chichester.

James, A.N., Lupton, A.R.R., 1978. Gypsum and anhydrite in foundations of hydraulic systems. Geotechnique 28, 249–272.

Jeschke, A.A., Vosbeck, K., Dreybrodt, W., 2001. Surface controlled dissolution rates of gypsum in aqueous solutions exhibit nonlinear dissolution kinetics. Geochim. Cosmochim. Acta 65, 27–34.

Keir, R.S., 1980. The dissolution kinetics of biogenic calcium carbonates in seawater. Geochim. Cosmochim. Acta 44, 241–252.

Klimchouk, A., Lowe, D., Cooper, A., Sauro, U. (Eds.), 1996. Int. J. Speleol. 25, Physical Speleology, special issue: Gypsum Karst of the World.

Lasaga, A.C., 1998. Kinetic Theory in the Earth Sciences. Princeton Ser. in Geochem., Princeton Univ. Press, Princeton.

Palmer, A.N., 1991. The origin and morphology of limestone caves. Geol. Soc. Amer. Bull. 103, 1–12.

Parkhurst, D.L., Appelo, C.A.J., 1999. User's guide to PHREEQC (version 2)—a computer program for speciation, reaction-path, advective transport and inverse geochemical calculations. U.S. Geol. Survey Water Resources Investigation. Report. 99-4259, Denver, Colorado.

Plummer, L.N., Wigley, T.M.L., 1976. The dissolution of calcite in CO_2 saturated solutions at 25 °C and 1 atmosphere total pressure. Geochim. Cosmochim. Acta 40, 191–202.

Plummer, L.N., Wigley, T.M.L., Parkhurst, D.L., 1978. The kinetics of calcite dissolution in CO_2–water systems at 5° to 60 °C and 0.0 to 1.0 atm CO_2. Am. J. Sci. 278, 179–216.

Svensson, U., Dreybrodt, W., 1992. Dissolution kinetics of natural calcite minerals in CO_2–water systems approaching calcite equilibrium. Chem. Geol. 100, 129–145.